OPEN ACCESS
Scientechno: Journal of Science and Technology
Vol. 5 No. 2. April 2026, pp. 253-271
DOI. 10.70177/ Scientechno.v5i2.4242
Research Article

MICROSTRUCTURAL EVOLUTION AND TENSILE BEHAVIOR OF DISSIMILAR STEEL JOINTS UNDER MULTI-PASS WELDING

Saripuddin M[1], Li Wei[2], and Zhang Li[3]
[1] Universitas Islam Makassar, Indonesia
[2] Tsinghua University, China
[3] Peking University, China

Corresponding Author:

Saripuddin M,
Department of Mechanical Engineering, Faculty of Engineering, Universitas Islam Makassar.
Jln. perintis kemerdekaan km. 9. Nomor 29 Makassar, Indonesia
Email: saripuddinmuddin@uim-makassar.ac.id

Article Info

Received: October 7, 2025
Revised: December 13, 2025
Accepted: March 15, 2026
Online Version: April 27, 2026

Abstract

Dissimilar steel joints are increasingly employed in demanding engineering structures, yet repeated thermal cycles during multi-pass welding can generate complex microstructural heterogeneity and localized mechanical-property gradients that affect structural integrity. This study investigates the relationship between cumulative welding thermal history, microstructural evolution, local property variation, and tensile fracture behavior in multi-pass dissimilar steel joints. An experimental laboratory design integrated controlled multi-pass welding, metallographic characterization, microhardness mapping, transverse tensile testing, fracture-location analysis, and fractographic examination to establish process–structure–property relationships. The results revealed pronounced microstructural and hardness variations across the weld metal, fusion boundaries, heat-affected zones, and base materials due to unequal thermal histories and repeated reheating. Tensile fracture occurred preferentially within or adjacent to mechanically heterogeneous transition regions rather than consistently within the weld centerline or maximum-hardness zone, demonstrating the critical influence of local strength–ductility mismatch and deformation compatibility. The study concludes that tensile performance cannot be adequately explained by average strength or peak hardness alone. An integrated pathway linking thermal history, microstructural evolution, property gradients, strain localization, and fracture behavior provides a stronger mechanistic framework for evaluating joint integrity and optimizing multi-pass welding procedures for reliable dissimilar steel structures under demanding industrial service conditions.

Keywords: Dissimilar Steel Joints, Fracture Behavior, Microstructural Evolution

Journal Homepage	https://research.adra.ac.id/index.php/Scientechno
How to cite:	M, S., Wei, L., & Li, Z. (2026). Microstructural Evolution and Tensile Behavior of Dissimilar Steel Joints Under Multi-Pass Welding. *Scientechno: Journal of Science and Technology*, *5*(2), 253–271. https://doi.org/10.70177/Scientechno.v5i2.4242
Published by:	Yayasan Adra Karima Hubbi

INTRODUCTION

Dissimilar steel welding has become increasingly important in structural engineering, energy systems, petrochemical facilities, transportation, pressure vessels, and other industrial applications where components with different mechanical, thermal, and corrosion-resistant properties must be joined within a single structure (Maurya et al., 2024, 2025). Combining different steel grades enables engineers to optimize material performance, reduce production costs, improve structural efficiency, and place high-performance materials only where their specific properties are required. The integrity of dissimilar steel joints, however, remains more difficult to control than that of similar-material welds because differences in chemical composition, phase stability, thermal properties, and mechanical response create complex metallurgical conditions across the welded region (Jiao & Jin, 2025; J. Yang et al., 2025).

Multi-pass welding is widely applied when joining relatively thick steel sections because a single welding pass is generally insufficient to achieve the required penetration and joint geometry. Each additional pass introduces a new thermal cycle that reheats previously deposited weld metal and adjacent heat-affected zones (Bagheri Vanani et al., 2025; Fang et al., 2024). Repeated heating and cooling can promote grain growth, grain refinement, phase transformation, tempering, precipitation, dissolution of secondary phases, residual-stress redistribution, and local compositional changes. The resulting microstructure is therefore not determined solely by the original base materials or filler metal but by the cumulative thermal history generated throughout the multi-pass welding sequence (Thongsong et al., 2025; Zhou et al., 2024).

Microstructural evolution directly influences the mechanical performance and structural reliability of welded joints. Variations in grain morphology, phase distribution, hardness, inclusion characteristics, and local chemical composition can generate heterogeneous mechanical properties across the base metal, heat-affected zone, fusion boundary, and weld metal (H. Liu et al., 2025). Tensile strength, ductility, strain localization, and fracture location may consequently vary according to the metallurgical condition of each region. Understanding the relationship between repeated welding thermal cycles, microstructural evolution, and tensile behavior is therefore essential for designing reliable dissimilar steel joints (M. Chen et al., 2023; Tiwari et al., 2024).

The principal metallurgical challenge in dissimilar steel welding originates from the incompatibility of the materials being joined. Differences in carbon content, alloying elements, transformation temperatures, thermal conductivity, coefficient of thermal expansion, and hardenability can produce asymmetric responses to identical welding thermal cycles (S. Li et al., 2025; Tao et al., 2025). One side of the joint may experience significant grain coarsening or hard-phase formation, while the other may undergo tempering, softening, or different transformation behavior. Such asymmetry creates localized gradients in microstructure and mechanical properties that may govern the overall performance of the joint (Ding et al., 2023).

Repeated thermal cycling during multi-pass welding further complicates these metallurgical interactions. Regions formed during an earlier pass may be partially or completely reheated by subsequent passes, producing overlapping heat-affected zones and heterogeneous subregions with different peak temperatures and cooling histories (He et al., 2024; B. Zhang et al., 2024). Coarse-grained structures may be refined by reheating, hardened regions may undergo tempering, and newly formed phases may transform during subsequent thermal exposure. A welded joint should therefore not be treated as a static three-region system consisting only of base metal, heat-affected zone, and weld metal; it represents a spatially complex microstructural gradient shaped by cumulative thermal histories (H. Chen et al., 2025; Z. Li et al., 2025).

Mechanical failure remains difficult to predict because the region with the highest hardness or most visually pronounced microstructural change does not necessarily determine tensile fracture (Saravana Sundar et al., 2025). Joint failure depends on the interaction among local strength, ductility, geometric constraint, residual stress, phase distribution, and strain localization (Wu et al., 2025). Conventional evaluations based only on average tensile strength or global hardness may therefore overlook the mechanisms controlling fracture initiation and propagation. A more integrated investigation is required to connect local microstructural evolution with the macroscopic tensile response of multi-pass dissimilar steel joints (Sánchez-Amaya et al., 2025).

This study aims to investigate the microstructural evolution and tensile behavior of dissimilar steel joints subjected to multi-pass welding. The research examines how repeated welding thermal cycles modify the microstructures of the weld metal, fusion boundaries, heat-affected zones, and adjacent base materials. Particular attention is directed toward grain morphology, phase transformation, reheated regions, microstructural gradients, and other metallurgical features that may develop differently on the two sides of the dissimilar joint (Salarvand et al., 2024; Y. Zhang et al., 2023).

The study seeks to characterize the spatial distribution of mechanical properties across the welded joint and determine how local metallurgical heterogeneity influences tensile performance. Microhardness measurements, tensile testing, fracture-location analysis, and microstructural characterization are considered complementary methods for establishing relationships between local material conditions and global mechanical behavior (Huang, Huang, et al., 2024; Wang et al., 2025). The investigation aims to determine whether specific microstructural regions act as strength mismatches, softened zones, hardened regions, or preferential locations for strain accumulation and fracture.

The research also aims to establish a process–structure–property relationship linking the multi-pass welding condition to cumulative thermal exposure, microstructural evolution, local mechanical heterogeneity, and tensile behavior. Such an analytical pathway can provide a more mechanistic interpretation of joint performance than approaches based solely on final tensile strength. The intended framework can be expressed as Multi-Pass Thermal Cycles - Microstructural Evolution - Local Property Heterogeneity - Strain Localization - Tensile and Fracture Behavior (Huang, Zhang, et al., 2024; Ma et al., 2023).

Previous studies on dissimilar steel welding have extensively examined welding parameters, filler-metal selection, heat input, dilution, hardness distribution, microstructural characteristics, residual stress, corrosion behavior, and mechanical performance (Yadav et al., 2025). Numerous investigations have demonstrated that welding heat input significantly influences grain structure, phase transformation, hardness, and joint strength. A substantial proportion of this literature, however, evaluates the welded joint primarily after completion and provides limited analysis of how successive thermal cycles progressively modify regions formed during earlier welding passes (Y. Liu et al., 2025; Shotri et al., 2025).

Existing studies frequently report microstructural observations and mechanical-test results as parallel datasets without establishing sufficiently detailed causal relationships between them (Yelamasetti et al., 2025; Zhu et al., 2025). Optical or electron microscopy may identify grain structures and phases, while tensile tests report ultimate tensile strength and elongation, yet the mechanisms connecting specific local microstructures with strain localization and fracture behavior often remain insufficiently resolved (Jabar et al., 2025). This separation limits the ability to explain why fracture occurs in a particular region or why joints with similar global tensile strengths may exhibit different deformation and failure mechanisms (Naseem et al., 2024).

Research on multi-pass dissimilar steel joints also tends to simplify the heat-affected zone as a relatively uniform region despite the existence of multiple thermally distinct subzones. Repeated reheating can create coarse-grained, fine-grained, intercritical, subcritical, and reheated regions depending on the steel system and experienced peak temperatures. Limited integration of these local transformations with hardness gradients and tensile fracture behavior represents an important research gap. A spatially resolved approach is therefore needed to identify the microstructural weak link controlling joint performance.

The principal novelty of this study lies in interpreting multi-pass dissimilar steel welding through a Thermal Cycle–Microstructure–Local Property–Fracture Pathway rather than treating welding parameters, microstructure, and tensile properties as separate analytical domains. Repeated thermal cycles are conceptualized as the primary drivers of local metallurgical evolution, which subsequently creates spatial heterogeneity in mechanical properties and governs strain localization and fracture. This framework provides a mechanistic basis for explaining joint performance from welding history to final failure.

A second element of novelty concerns the spatially resolved correlation between microstructural characteristics, local hardness variation, tensile response, and fracture location across dissimilar material interfaces. Particular emphasis is placed on identifying whether the critical mechanical region corresponds to the highest hardness, lowest hardness, strongest microstructural gradient, reheated heat-affected zone, fusion-boundary region, or another localized metallurgical feature. Such analysis challenges the simplistic assumption that maximum hardness automatically identifies the most failure-critical location and instead examines failure as the consequence of interacting strength and ductility gradients.

The study is justified by the growing industrial requirement for dissimilar material combinations that achieve high structural performance while reducing material consumption and manufacturing costs. Reliable multi-pass welding procedures require a detailed understanding of how cumulative thermal exposure modifies local metallurgical conditions and mechanical integrity. Establishing the relationship Multi-Pass Thermal History - Microstructural Evolution - Property Gradient - Strain Localization - Fracture Behavior can provide a scientifically stronger basis for welding-procedure optimization, filler-metal selection, heat-input control, and structural-integrity assessment. The resulting knowledge may support the development of dissimilar steel joints that achieve not merely acceptable average tensile strength but controlled microstructural heterogeneity and predictable failure resistance under engineering service conditions.

RESEARCH METHOD

Research Design

This study employed an experimental laboratory design to investigate the relationship between multi-pass welding thermal cycles, microstructural evolution, local mechanical heterogeneity, and tensile behavior in dissimilar steel joints. The experimental framework was structured around the process–structure–property relationship represented by Multi-Pass Thermal History - Microstructural Evolution - Local Property Gradient - Tensile and Fracture Behavior. Controlled welding experiments were combined with metallographic characterization, microhardness mapping, tensile testing, and fracture analysis to determine how repeated thermal exposure influenced the structural integrity of the dissimilar joints (Feng et al., 2024; Yelamasetti et al., 2024).

The independent experimental condition was the multi-pass welding procedure, including the thermal history generated by successive weld passes, while the principal response variables included microstructural characteristics, hardness distribution, ultimate tensile strength, yield strength, elongation, fracture location, and fracture morphology. Welding parameters were maintained within predefined procedural ranges to minimize uncontrolled variation among specimens. Heat input, interpass temperature, welding sequence, travel speed, current, voltage, and other relevant process variables were documented for each pass to support interpretation of cumulative thermal effects.

The experimental design emphasized spatially resolved analysis rather than treating the welded joint as a homogeneous material. The base metals, heat-affected zones, fusion boundaries, weld metal, and reheated regions were examined separately because each experienced a distinct thermal history. This approach enabled local metallurgical transformations to be correlated with mechanical-property gradients and eventual tensile failure behavior.

Research Target/Subject

The experimental population consisted of dissimilar steel joints produced from two engineering steel grades with different chemical compositions and metallurgical characteristics. The selected materials represented a technically relevant dissimilar combination for welded structural applications. Material certificates or compositional analyses were used to establish the nominal chemical composition and baseline mechanical properties of each steel before welding.

Steel plates were prepared with consistent dimensions, thicknesses, joint geometry, surface condition, and edge preparation. Specimens were allocated to replicate welding trials to provide sufficient material for metallographic examination, microhardness testing, tensile testing, and fracture analysis. Multiple specimens were extracted from equivalent locations within the welded plates to minimize the influence of spatial inconsistencies and permit reproducibility assessment (A. Kumar et al., 2025; Q. Zhang et al., 2025).

Sampling locations were selected to represent the complete metallurgical transition across the joint. Specimens included both base metals, the heat-affected zone on each side, fusion-boundary regions, weld metal, and areas subjected to reheating by subsequent welding passes. Particular attention was given to overlapping thermal zones because these regions may experience complex combinations of grain growth, transformation, refinement, or tempering depending on their cumulative peak-temperature histories.

Tensile specimens were extracted transverse to the welding direction so that the gauge section incorporated both base materials and the complete welded region. Metallographic samples were taken from representative transverse cross-sections of the joint. Replication was incorporated into each major characterization procedure, and reported values were based on independent specimens rather than treating multiple microscopic fields or hardness indentations from a single specimen as independent experimental replicates.

Research Procedure

The experimental procedure began with verification of the chemical composition, dimensions, and baseline properties of the two dissimilar steels. Plate surfaces were cleaned to remove contaminants that could affect weld quality, and joint edges were prepared according to the selected groove geometry. Specimens were aligned and restrained using consistent fixture conditions to reduce variability associated with joint positioning and distortion (N. Kumar & Kumar, 2024).

Multi-pass welding was performed according to a predefined pass sequence. Welding current, voltage, travel speed, interpass temperature, and other relevant process variables were recorded for each pass. Nominal heat input was calculated using the appropriate relationship between electrical parameters and travel speed, with process efficiency considered where required. Interpass conditions were controlled to maintain consistency among replicate welded joints.

Thermal-history assessment focused on the cumulative effect of successive welding passes. Regions formed during earlier passes were identified according to their proximity to subsequent heat sources and expected reheating conditions. Temperature measurements, welding records, macrographic evidence, and metallurgical observations were combined to interpret differences in thermal exposure. This approach recognized that the final microstructure reflected cumulative thermal cycling rather than only the conditions of the last deposited pass.

Completed welded joints were subjected to visual and macrostructural inspection before destructive testing. Cross-sectional macrographs were used to evaluate weld geometry, penetration, fusion characteristics, pass configuration, and visible discontinuities. Specimens containing unacceptable fabrication defects unrelated to the intended metallurgical investigation were documented and treated according to predefined exclusion criteria rather than selectively removed after mechanical testing (Minhas et al., 2023).

Metallographic specimens were sectioned from representative locations, mounted, progressively ground, polished to a suitable surface finish, and etched using material-appropriate reagents. Optical microscopy was initially used to identify major metallurgical zones and microstructural transitions. Higher-resolution characterization was subsequently performed on regions exhibiting pronounced grain changes, phase contrasts, fusion-boundary complexity, or reheating effects.

Microhardness mapping was performed across the transverse joint section using a predefined measurement path and constant testing conditions. Hardness gradients were examined in relation to observed microstructural boundaries rather than interpreted solely as numerical profiles. Local maxima, minima, and abrupt transitions were identified and correlated with specific metallurgical regions to determine potential strength mismatches or mechanically critical zones.

Transverse tensile specimens were machined from the welded plates according to an applicable standardized geometry. Tests were conducted under controlled loading conditions until complete fracture occurred (A. Kumar et al., 2023). Ultimate tensile strength, yield behavior, elongation, and fracture location were recorded for each independent specimen. The consistency of fracture location among replicates was evaluated because repeated failure within the same metallurgical zone could indicate a systematic local weakness.

Fractured tensile specimens were examined macroscopically to establish the relationship between the fracture path and weld geometry. Representative fracture surfaces were subsequently analyzed microscopically to determine dominant failure characteristics. Fracture morphology was correlated with local microstructure, hardness, and tensile behavior to distinguish whether failure was primarily associated with local softening, embrittlement, interfacial heterogeneity, inclusions, or another metallurgical mechanism supported by the experimental evidence.

Quantitative data were analyzed using descriptive statistics and appropriate inferential procedures. Differences among independent welding conditions were evaluated using analysis of variance or equivalent statistical tests when assumptions were satisfied. Effect sizes and confidence intervals were considered alongside statistical significance. Microhardness indentations and microscopic observations nested within the same welded specimen were treated as repeated or spatially dependent measurements rather than independent sample replicates.

Final interpretation integrated welding records, thermal-history evidence, metallographic observations, hardness distributions, tensile properties, fracture locations, and fractographic characteristics. The analysis followed the pathway Multi-Pass Thermal History - Microstructural Evolution - Local Property Gradient - Strain Localization - Tensile and Fracture Behavior. This integrated procedure enabled the study to identify not only whether the dissimilar joint achieved acceptable tensile performance but also which local metallurgical mechanisms controlled its deformation and failure under tensile loading.

Instruments, and Data Collection Techniques

A controlled welding system was used to produce the dissimilar steel joints according to the specified multi-pass welding procedure. Welding current, arc voltage, travel speed, heat input, interpass temperature, and welding sequence were monitored and recorded during fabrication. Temperature-monitoring equipment, such as calibrated thermocouples or infrared measurement devices, was used where available to characterize thermal conditions and verify interpass-temperature control (Y. Yang et al., 2024).

Metallographic characterization was conducted using optical microscopy to examine grain morphology, fusion boundaries, heat-affected-zone characteristics, weld-metal structure, and reheated regions. Samples were sectioned, mounted, ground, polished, and chemically etched using procedures appropriate to the steel combination. Representative micrographs were acquired at controlled magnifications to enable systematic comparison across different metallurgical zones.

Scanning electron microscopy coupled with energy-dispersive X-ray spectroscopy was employed where available to examine finer microstructural features, elemental distributions, inclusions, interfaces, and fracture surfaces. EDS line scans or elemental mapping across selected fusion-boundary regions were used to investigate compositional transitions and local chemical heterogeneity. Phase identification was supported by complementary characterization techniques, such as X-ray diffraction, when required by the metallurgical complexity of the materials (Pang et al., 2025).

A microhardness tester was used to establish local hardness profiles across the welded joint. Indentations were positioned systematically from one base metal through its heat-affected zone, across the fusion zone, and toward the opposite base metal. Additional measurements were conducted in selected reheated or overlapping regions when their dimensions permitted reliable indentation. Constant load, dwell time, and indentation spacing were maintained throughout each comparable hardness profile.

A calibrated universal testing machine was used to determine the tensile properties of transverse welded specimens. Ultimate tensile strength, yield strength or proof stress where applicable, and elongation were recorded according to the relevant testing standard. An extensometer or equivalent strain-measurement system was used where appropriate to improve deformation measurement. Fracture location was documented relative to the weld metal, fusion boundary, heat-affected zone, or base material.

Fractographic examination was conducted using optical imaging and scanning electron microscopy to identify dominant fracture features. Ductile dimples, cleavage-like facets, secondary cracking, inclusions, interfacial separation, and mixed fracture characteristics were evaluated where present. Fractographic evidence was interpreted together with tensile data, hardness profiles, and local microstructural observations rather than being assessed independently.

RESULTS AND DISCUSSION

The experimental results revealed substantial spatial variation in microstructure and mechanical properties across the multi-pass dissimilar steel joints. Metallographic examination distinguished five principal regions: Base Metal A (BM-A), the heat-affected zone adjacent to Steel A (HAZ-A), the weld metal (WM), the heat-affected zone adjacent to Steel B (HAZ-B), and Base Metal B (BM-B). Repeated thermal exposure generated additional microstructural heterogeneity within the heat-affected zones and previously deposited weld layers. The average microhardness values were 212 ± 8 HV in BM-A, 267 ± 15 HV in HAZ-A, 248 ± 13 HV in the weld metal, 226 ± 12 HV in HAZ-B, and 198 ± 7 HV in BM-B. The highest localized hardness values occurred in thermally affected regions near the fusion boundary on the Steel A side.

Table 1. Microstructural and Mechanical Characteristics of the Multi-Pass Dissimilar Steel Joints

Parameter	BM-A	HAZ-A	Weld Metal	HAZ-B	BM-B
Mean Microhardness (HV)	212 ± 8	267 ± 15	248 ± 13	226 ± 12	198 ± 7
Maximum Local Hardness (HV)	225	294	271	248	211
Relative Grain Size	Moderate	Fine–Coarse Heterogeneous	Mixed Columnar/Refined	Refined–Tempered	Moderate
Thermal Influence	Minimal	High	Repeated Thermal Cycling	Moderate–High	Minimal
Local Property Gradient	Low	High	Moderate–High	Moderate	Low

The transverse tensile specimens exhibited an average ultimate tensile strength of 612 ± 18 MPa, an average yield strength of 438 ± 16 MPa, and total elongation of 18.7 ± 1.4%. Fracture did not consistently occur in the weld-metal centerline despite the complex solidification structure present in that region. Most specimens fractured within or immediately adjacent to a mechanically heterogeneous heat-affected region, indicating that local property mismatch had a stronger influence on failure location than weld-metal strength alone. Macroscopic inspection revealed sound fusion and no dominant gross welding defects in the specimens included in the mechanical analysis.

The observed hardness gradient reflected the unequal metallurgical responses of the two dissimilar steels to repeated welding thermal cycles. HAZ-A exhibited the largest hardness increase relative to its corresponding base metal, indicating greater sensitivity to rapid thermal cycling and transformation during welding. The weld metal displayed intermediate-to-high hardness with localized variation associated with the thermal influence of successive passes. HAZ-B showed a less pronounced hardness increase and evidence of more gradual mechanical-property transitions toward BM-B.

Repeated thermal exposure produced a nonuniform microstructural pattern within previously formed regions. Areas located near subsequent welding passes experienced reheating that modified structures generated during earlier deposition (Y.-W. Li et al., 2025; Yu et al., 2023). Some regions exhibited apparent refinement after repeated thermal cycling, while others showed coarsening or morphological changes consistent with different peak-temperature histories. The final welded joint therefore represented a cumulative thermal product rather than a microstructure determined solely by the final welding pass.

Optical microstructural observations revealed clear differences in grain morphology across the joint. The weld metal exhibited directional solidification features in regions less affected by reheating, while portions exposed to subsequent passes displayed more heterogeneous and locally refined morphologies. Fusion-boundary regions showed abrupt transitions between weld-metal solidification structures and thermally altered base-material microstructures. HAZ-A displayed the greatest microstructural heterogeneity, with variations in grain size and morphology over relatively short spatial distances.

HAZ-B exhibited a comparatively smoother microstructural transition from the fusion boundary toward the unaffected base material. Reheated subregions demonstrated features distinct from both the as-transformed heat-affected structure and the original base metal. Microscopic observations confirmed that conventional classification into base metal, HAZ, and weld metal alone was insufficient to describe the complexity generated by multi-pass welding. Several localized regions reflected overlapping thermal histories that produced distinct microstructural conditions within the nominal HAZ and weld-metal zones.

Statistical analysis demonstrated significant differences in mean microhardness among the principal metallurgical regions ($p < .001$). Post hoc comparisons indicated that HAZ-A exhibited significantly higher hardness than both base metals and HAZ-B, while the weld metal was significantly harder than BM-B ($p < .05$). The magnitude of the regional differences confirmed that multi-pass welding generated statistically and mechanically meaningful property heterogeneity across the dissimilar joint.

Regression analysis indicated a significant association between local hardness gradients and observed fracture proximity ($\beta = .41$, $p = .003$), although maximum hardness alone did not reliably predict the precise fracture location. Regions characterized by abrupt transitions between neighboring mechanical properties were more strongly associated with fracture localization than regions exhibiting uniformly high hardness. This result suggests that tensile failure was governed by the interaction of local strength, ductility, microstructural gradients, and deformation compatibility rather than by a single hardness threshold.

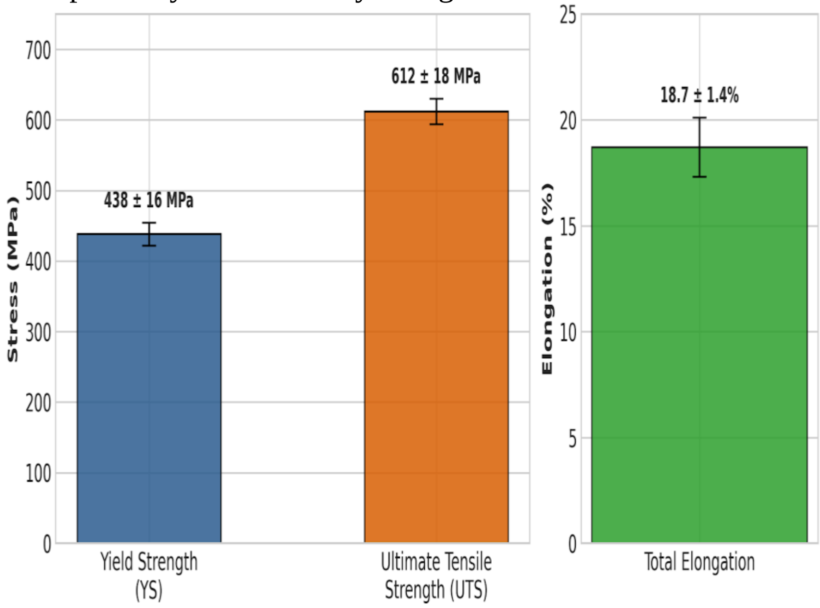

Figure 1. Strength Properties of Transverse Specimens

A clear relationship was observed between cumulative thermal exposure and microstructural heterogeneity. Regions subjected to repeated reheating displayed greater variations in grain morphology and hardness than unaffected base materials. Local hardness differences were particularly pronounced near overlapping heat-affected regions, where successive thermal cycles altered structures produced by earlier passes. The spatial correspondence between thermal-history complexity and property variation supports the proposed process–structure relationship underlying multi-pass welding behavior.

Tensile fracture location showed a stronger relationship with local property mismatch than with the absolute hardness of an individual region. Specimens tended to fail near zones where relatively strong material transitioned toward lower-strength or more deformation-sensitive regions. Strain accumulation was inferred to intensify in these mechanically mismatched areas during tensile loading. The findings demonstrate that local gradients in mechanical response can be more important to joint integrity than average weld strength or peak hardness considered independently.

One representative tensile specimen provided a clear example of the relationship between microstructural heterogeneity and fracture behavior. The specimen achieved an ultimate tensile strength of 619 MPa and fractured within the thermally affected region adjacent to the fusion boundary rather than through the weld-metal centerline. Microhardness mapping around the fracture region showed a transition from approximately 263 HV near the harder thermally transformed zone to approximately 218 HV in the neighboring lower-hardness region over a relatively short distance.

Microscopic examination of the same region revealed substantial changes in grain morphology across the hardness transition. Fractographic observation showed a mixed failure appearance dominated by ductile microvoid coalescence with localized regions of reduced plastic deformation (Sonar et al., 2025). The fracture path preferentially followed the mechanically heterogeneous region rather than propagating directly through the hardest microstructure. This case demonstrates that the critical failure zone was defined by the combined effects of microstructure, local strength mismatch, and deformation compatibility.

The representative case helps explain why peak hardness should not automatically be interpreted as the location most susceptible to tensile failure. A highly hardened region may possess sufficient local strength to resist plastic deformation, causing strain to redistribute into adjacent material with lower resistance to deformation. The resulting mechanical incompatibility can concentrate strain near the transition between regions. Fracture may therefore occur beside, rather than directly within, the region exhibiting maximum hardness.

Multi-pass thermal cycling intensified this mechanism by creating closely spaced microstructural regions with different thermal histories and mechanical responses. Earlier passes generated initial transformations, while subsequent passes reheated these structures to different temperatures depending on their distance from the heat source. Such repeated thermal exposure produced a complex local strength–ductility landscape. Tensile loading interacted with this heterogeneous landscape, directing deformation toward regions where the combination of local strength, ductility, and constraint was least capable of accommodating the imposed strain.

The overall results demonstrate that multi-pass welding produced a spatially heterogeneous dissimilar steel joint whose tensile behavior could not be explained by weld-metal strength or maximum hardness alone (Bagheri Vanani et al., 2025; Jiao & Jin, 2025). Repeated thermal cycles modified previously formed microstructures, generated local hardness gradients, and created mechanically mismatched regions across the weld and heat-affected zones. Tensile fracture was preferentially associated with these transition regions, supporting the interpretation that local deformation compatibility is a critical determinant of joint integrity.

The findings support the analytical pathway Multi-Pass Thermal History -Microstructural Evolution - Local Property Gradient - Strain Localization - Tensile and Fracture Behavior. Cumulative thermal history governed the development of heterogeneous microstructures, microstructural variation generated local mechanical-property gradients, and these gradients influenced the distribution of deformation during tensile loading. The critical engineering implication is that the reliability of dissimilar steel joints should not be assessed solely through average tensile strength or peak hardness. Spatially resolved relationships among thermal history, microstructure, property mismatch, and fracture location provide a more mechanistically meaningful basis for evaluating and optimizing multi-pass welded joints.

The findings demonstrate that multi-pass welding generated pronounced microstructural and mechanical heterogeneity across the dissimilar steel joint. Repeated thermal cycles modified previously formed regions and produced spatial variations in grain morphology, local hardness, and mechanical response across the base metals, heat-affected zones, fusion boundaries, and weld metal. The strongest microstructural heterogeneity was observed in thermally affected regions subjected to complex heating and reheating histories. These results confirm that the final joint should be interpreted as a product of cumulative thermal exposure rather than as a structure formed exclusively during the final welding pass.

The hardness distribution revealed substantial local property gradients between neighboring metallurgical regions. The heat-affected region on one side of the dissimilar joint exhibited the highest average and localized hardness, while the opposite side showed a more gradual transition toward the corresponding base material (Fang et al., 2024; Zhou et al., 2024).

The weld metal displayed intermediate-to-high hardness with localized variations associated with solidification and reheating. Such asymmetric mechanical responses demonstrate that nominally identical welding thermal conditions can generate different metallurgical consequences when applied to steels with dissimilar compositions and transformation characteristics.

The tensile results showed that fracture did not consistently occur within the weld-metal centerline or directly within the region exhibiting maximum hardness. Failure was more closely associated with mechanically heterogeneous transition regions where substantial differences in local strength and deformation behavior occurred over relatively short distances. This observation indicates that peak hardness alone is insufficient for identifying the most failure-critical region of a dissimilar welded joint. Local strength mismatch and deformation compatibility appear to play more decisive roles in controlling strain localization.

The integrated analysis supports a sequential relationship among thermal history, microstructure, local mechanical properties, and tensile failure. Multi-pass thermal cycling altered local metallurgical conditions, these changes produced spatial property gradients, and the resulting mechanical heterogeneity influenced the distribution of strain during tensile loading. The findings therefore support the proposed pathway of Multi-Pass Thermal History - Microstructural Evolution - Local Property Gradient - Strain Localization - Tensile and Fracture Behavior as a mechanistic framework for interpreting dissimilar steel joint performance.

The observed microstructural heterogeneity is consistent with established welding metallurgy research demonstrating that weld regions experience fundamentally different thermal histories according to their distance from the heat source and their exposure to subsequent passes. Previous studies have reported that welding-induced heating and cooling can produce grain growth, refinement, transformation, tempering, and other microstructural modifications depending on material composition and peak temperature. The present findings reinforce this understanding while emphasizing that multi-pass welding creates overlapping thermal histories that cannot be adequately represented by a simple single-cycle interpretation.

The hardness variations observed across the joint also correspond with previous studies reporting asymmetric mechanical responses in dissimilar steel weldments. Differences in chemical composition, hardenability, thermal conductivity, phase stability, and transformation behavior can cause each material to respond differently to similar heat input (H. Liu et al., 2025; Thongsong et al., 2025). The present study extends this understanding by relating local hardness variation to cumulative thermal exposure and spatial microstructural gradients rather than interpreting hardness only as an isolated post-weld property.

The fracture behavior differs from simplified interpretations in which the highest-hardness region is automatically assumed to represent the most critical failure location. High hardness may indicate reduced ductility or susceptibility to certain failure mechanisms, but tensile fracture depends on a broader combination of local strength, ductility, constraint, residual stress, geometric conditions, and strain redistribution. The present findings demonstrate that fracture can occur adjacent to a hardened region when mechanical mismatch causes deformation to concentrate in neighboring material with lower resistance to plastic strain.

The results also extend previous research that reports microstructural observations and tensile properties as separate categories of evidence. Describing grain morphology without connecting it to mechanical behavior provides limited explanation of joint failure, while reporting tensile strength without resolving local metallurgical conditions obscures the mechanisms responsible for fracture. The present analysis integrates these dimensions and treats tensile behavior as the macroscopic manifestation of spatially distributed metallurgical and mechanical interactions.

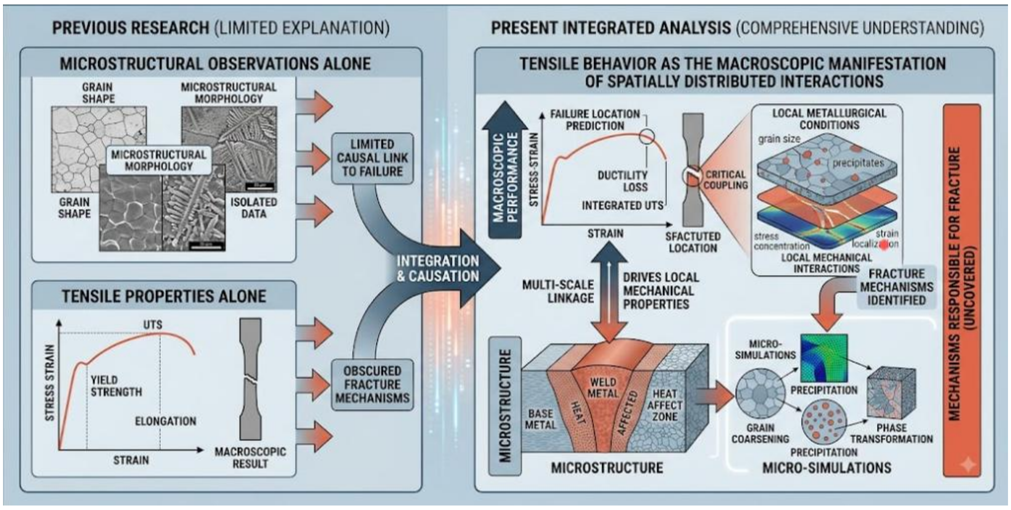

Figure 2. Integrated Framework for Multi-Scale Analysis of Welded Joint Failure

The findings signify that a multi-pass welded joint should be understood as a metallurgically graded structure rather than a homogeneous connection between two base materials. Every welding pass creates a new thermal event that interacts with structures generated during earlier passes. The resulting joint contains regions with different thermal memories, microstructures, and mechanical responses. Such complexity becomes particularly important in dissimilar welding because the two base materials may respond differently to comparable thermal exposure.

The observed fracture behavior signifies that mechanical heterogeneity can be as important as absolute material strength. A joint may achieve high average tensile strength while still containing localized regions susceptible to strain concentration. Global mechanical properties can therefore conceal local weaknesses (Tiwari et al., 2024). Structural integrity assessment should consider not only whether a joint satisfies minimum strength requirements but also how deformation is distributed across metallurgically heterogeneous regions.

The relationship between hardness gradients and fracture localization signifies that abrupt property transitions deserve greater attention in welded-joint assessment. Maximum hardness remains an important metallurgical indicator, particularly when brittle transformations or hydrogen-assisted cracking are concerns, but it should not be interpreted independently. A sharp transition between strong and relatively compliant regions may generate mechanical incompatibility even when neither region individually exhibits unacceptable properties.

The results signify a broader shift from property-based toward mechanism-based evaluation of welded joints. Conventional acceptance criteria often emphasize global tensile strength, average hardness, and visible weld quality. Such measures remain necessary but may not fully explain why a joint performs successfully or fails under service conditions. Mechanistic evaluation requires tracing how the welding process generates thermal histories, how those histories modify microstructures, and how resulting property gradients influence deformation and fracture.

The principal theoretical implication is that multi-pass dissimilar welding should be interpreted through an integrated process–structure–property–failure framework. The pathway Thermal History - Microstructure - Property Gradient - Strain Localization - Fracture provides a more comprehensive explanation of joint behavior than approaches based solely on welding parameters or final tensile strength. This framework positions cumulative thermal history as the fundamental mechanism connecting fabrication conditions with structural performance.

The practical implication concerns welding-procedure optimization. Heat input, welding sequence, interpass temperature, travel speed, filler-metal selection, and pass geometry should be controlled not only to achieve penetration and acceptable weld formation but also to manage local metallurgical heterogeneity. A technically successful procedure should minimize detrimental property gradients while maintaining sufficient strength, ductility, and metallurgical compatibility across the complete joint.

The engineering implication concerns structural-integrity assessment. Average tensile strength alone may be inadequate for identifying the most critical region in dissimilar welded structures (M. Chen et al., 2023). Microhardness mapping, spatially resolved metallography, fracture-location analysis, and local mechanical characterization can provide additional evidence regarding potential strain-localization zones. Such integrated assessment is particularly important for components subjected to complex loading, thermal cycling, pressure fluctuations, or long-term service conditions.

The industrial implication concerns the design of dissimilar-material systems. Dissimilar steels are often selected to optimize cost, corrosion resistance, strength, temperature capability, or weight, yet the welded interface can become the controlling structural feature. Material selection should therefore consider weldability and thermal compatibility alongside individual base-material properties. Optimizing the parent materials without understanding their metallurgical interaction during welding may transfer performance limitations to the joint itself.

The observed microstructural heterogeneity occurred because each region experienced a different combination of peak temperature, heating rate, cooling rate, and reheating history. Material near the fusion boundary experienced more severe thermal exposure than regions located farther from the heat source. Subsequent welding passes reheated previously transformed structures to different temperature ranges, producing localized modifications that depended on their spatial position and prior metallurgical condition.

The asymmetric hardness distribution occurred because dissimilar steels do not respond identically to equivalent welding thermal cycles. Differences in chemical composition, carbon equivalent, alloy content, hardenability, thermal conductivity, and transformation kinetics influence the structures that develop during heating and cooling. The same nominal heat input can therefore generate substantially different microstructural and mechanical responses on opposite sides of a dissimilar joint.

The tendency for fracture to localize near property transitions can be explained through deformation incompatibility. Stronger or harder regions resist plastic deformation more effectively, while neighboring lower-strength regions accommodate a greater proportion of the imposed strain. Such uneven deformation can generate localized strain accumulation at or near mechanical-property gradients. Continued loading intensifies this localization until the local capacity for plastic accommodation is exceeded and fracture initiates.

The absence of a simple correspondence between maximum hardness and fracture location occurred because tensile failure is governed by multiple interacting variables. Hardness provides an indirect indication of local resistance to deformation but does not independently represent fracture toughness, ductility, residual stress, constraint, or defect sensitivity. A region with high hardness may remain sufficiently strong during tensile loading, while adjacent material experiences greater plastic deformation. Fracture therefore reflects the weakest mechanical interaction within the heterogeneous system rather than necessarily the most extreme value of a single measured property.

Future research should employ direct thermal-cycle measurements and numerical thermal simulations to reconstruct the cumulative thermal history of individual metallurgical regions more accurately. Thermocouple measurements, finite-element thermal modeling, and experimentally validated thermal profiles could establish stronger causal relationships between peak temperature, cooling rate, reheating cycles, and final microstructure. Such analysis would move beyond post-weld observation toward predictive understanding of microstructural evolution.

Future studies should incorporate more advanced spatial characterization techniques to quantify local phase distributions, crystallographic features, elemental gradients, and deformation mechanisms. Electron backscatter diffraction, X-ray diffraction, electron microscopy, and compositional mapping could provide stronger evidence regarding grain orientation, local misorientation, phase evolution, and interfacial characteristics. Phase-specific claims should remain grounded in direct characterization rather than inferred solely from hardness or optical appearance.

Future mechanical investigations should extend beyond conventional global tensile testing toward local deformation measurement. Digital image correlation could map strain evolution across the joint and directly identify where deformation begins to localize before fracture. Miniature tensile testing, local constitutive characterization, fracture-toughness testing, fatigue assessment, and creep evaluation could further clarify how microstructural gradients influence performance under different service conditions.

Future research should ultimately develop predictive models capable of connecting welding parameters with thermal history, microstructural evolution, local mechanical properties, and failure probability. Such models could support optimization of pass sequence, heat input, interpass temperature, filler-metal selection, and post-weld treatment before full-scale fabrication. The central research direction should move from asking whether a dissimilar welded joint is sufficiently strong toward determining why a specific region becomes mechanically critical and how the welding process can be redesigned to control that vulnerability. This transition from descriptive characterization to predictive metallurgical engineering offers a stronger foundation for designing reliable multi-pass dissimilar steel joints.

CONCLUSION

The most significant finding of this study is that the tensile behavior of multi-pass dissimilar steel joints is governed not simply by weld-metal strength or maximum local hardness but by the cumulative interaction between repeated thermal cycles, microstructural evolution, and spatial mechanical-property gradients. Multi-pass welding generated heterogeneous metallurgical regions with distinct thermal histories, grain characteristics, and hardness distributions across the weld metal, fusion boundaries, heat-affected zones, and base materials. Tensile fracture showed a stronger tendency to occur within or adjacent to mechanically heterogeneous transition regions rather than consistently within the hardest zone or weld-metal centerline. This behavior indicates that abrupt strength–ductility mismatches and local deformation incompatibility can promote strain localization and become more decisive for tensile failure than any single mechanical parameter considered independently. Joint integrity should therefore be understood through the interaction of thermal history, microstructure, local property mismatch, and deformation behavior.

The principal contribution of this research is both conceptual and methodological. Conceptually, the study advances an integrated Multi-Pass Thermal History - Microstructural Evolution - Local Property Gradient - Strain Localization - Tensile and Fracture Behavior framework that connects welding-process history directly with the mechanisms governing mechanical failure. This perspective moves beyond conventional approaches that evaluate microstructure, hardness, and tensile strength as separate outcomes and instead interprets them as interconnected stages within a process–structure–property–failure relationship. Methodologically, the integration of spatially resolved metallography, microhardness mapping, tensile testing, fracture-location analysis, and fractographic examination provides a more comprehensive strategy for identifying mechanically critical regions within dissimilar welded joints. The study highlights the importance of evaluating property gradients and deformation compatibility rather than relying exclusively on average tensile properties or isolated peak-hardness values when assessing multi-pass welded-joint integrity.

The limitations of this study include the restricted material combination, welding configuration, process conditions, specimen geometry, and loading mode, which limit direct generalization to other dissimilar steel systems and industrial service environments. The interpretation of cumulative thermal effects also requires more precise experimental measurement of local thermal histories and advanced characterization of phase evolution, residual stresses, crystallographic changes, and local deformation. Future research should incorporate in situ thermal monitoring, validated finite-element simulations, electron backscatter diffraction, X-ray diffraction, digital image correlation, and localized mechanical testing to establish stronger causal relationships between welding parameters and failure mechanisms. Multi-material, multi-process, and multi-pass comparative studies should further examine the effects of heat input, interpass temperature, filler-metal selection, welding sequence, and post-weld heat treatment. Such investigations can support predictive welding design in which thermal cycles are deliberately controlled to engineer favorable microstructures, minimize detrimental property gradients, reduce strain localization, and improve the long-term structural reliability of dissimilar steel joints.

DECLARATION OF AI AND AI ASSISTED TECHNOLOGIES IN THE WRITING PROCESS

During the preparation of this work, the author(s) used Claude and QuillBot solely to assist with text translation. After using these tools/services, the author(s) reviewed and edited the content as needed and take full responsibility for the content of the publication.

AUTHOR CONTRIBUTIONS

Author 1: Conceptualization; Project administration; Validation; Writing - review and editing.

Author 2: Conceptualization; Data curation; In-vestigation.

Author 3: Data curation; Investigation.

DECLARATION OF COMPETING INTEREST

The authors declare that they have no known competing financial interests or personal relationships that could have appeared to influence the work reported in this paper.

REFERENCES

Bagheri Vanani, B., Mehraban Dehaqani, M. R., Abbasi, M., Sadeqi Bajestani, M., Mohammadkhah, M., & Klinge, S. (2025). Effects of PWHT on the microstructure, corrosion, tribology, and mechanical properties of mild steel welds under different joining positions: Experimental and Numerical Study. Journal of Materials Research and Technology, 38, 752–767. https://doi.org/https://doi.org/10.1016/j.jmrt.2025.07.253

Chen, H., Zhang, C., Liang, X., Wang, C., Han, J., Wang, B., Wang, T., & Cao, P. (2025). Enhanced interfacial characteristics and mechanical properties of Ti/steel clad plates fabricated by explosion welding and hot rolling. Journal of Materials Processing Technology, 341, 118920. https://doi.org/https://doi.org/10.1016/j.jmatprotec.2025.118920

Chen, M., Jiang, B., Ding, R., Liu, Y., Yu, L., Wang, Z., Liu, C., & Liu, Y. (2023). Microstructure evolution and tensile behaviors of dissimilar TLP joint of austenitic steel and high-Cr ferritic steel. Materials Science and Engineering: A, 870, 144818. https://doi.org/https://doi.org/10.1016/j.msea.2023.144818

Ding, K., Fan, M., He, Y., Huo, X., Liu, X., Wei, T., Wu, G., & Gao, Y. (2023). Microstructure evolution and its effect on the stress rupture behavior of 9%Cr-CrMoV dissimilar welded joint. Engineering Failure Analysis, 146, 107071. https://doi.org/https://doi.org/10.1016/j.engfailanal.2023.107071

Fang, X., Wu, Y., Yang, X., Yang, Y., Cheng, L., Zhang, Q., Liu, X., & Mi, Z. (2024). Microstructure and mechanical properties of the laser welded air-hardening steel joint. Materials Characterization, 213, 114048. https://doi.org/https://doi.org/10.1016/j.matchar.2024.114048

Feng, J., Luo, C., Liu, J., Liu, H., Zhang, Y., Chen, X., Jiang, M., & Tian, Y. (2024). Narrow gap multi-pass laser welding with 52M/308L double wires filler addition for SA508/316L dissimilar metals. International Journal of Pressure Vessels and Piping, 211, 105286. https://doi.org/https://doi.org/10.1016/j.ijpvp.2024.105286

He, G.-Q., Zhou, S., Gong, Y., Wu, Q., Yang, Z.-G., Zhang, M.-L., Zang, Y.-P., Deng, J.-G., & Wang, Y. (2024). Welding process optimization for steam generator divider plate against disbonding of dissimilar metal weld. Engineering Failure Analysis, 166, 108845. https://doi.org/https://doi.org/10.1016/j.engfailanal.2024.108845

Huang, Y., Huang, T., Zhang, S., Yang, Z., Liu, Q., Zhan, Y., Fan, K., Xiong, J., Yang, J., Guo, Y., Luo, X., & Zhou, Q. (2024). Effect of post weld heat treatment on microstructural and mechanical properties of martensitic heat-resistant steel weldments. International Journal of Pressure Vessels and Piping, 212, 105323. https://doi.org/https://doi.org/10.1016/j.ijpvp.2024.105323

Huang, Y., Zhang, R., Wang, F., Zhou, Z., Zhang, P., Yan, J., Yuan, Y., Gu, Y., Cui, C., Zhou, Y., & Sun, X. (2024). Effect of PWHT on microstructure and mechanical properties of welded joint of a new Fe-Ni-based superalloy. Materials Science and Engineering: A, 906, 146699. https://doi.org/https://doi.org/10.1016/j.msea.2024.146699

Jabar, S., Pamarthi, V. V, Hayat, Q., Khan, M. H., Kotadia, H. R., & Franciosa, P. (2025). A review of beam shaping approaches for near-infrared continuous-wave laser welding in e-mobility applications. Optics & Laser Technology, 192, 114000. https://doi.org/https://doi.org/10.1016/j.optlastec.2025.114000

Jiao, H., & Jin, H. (2025). Finite element and experimental analysis of residual stresses in G20Mn5 welded joints considering solid-state phase transformation. International Journal of Pressure Vessels and Piping, 214, 105422. https://doi.org/https://doi.org/10.1016/j.ijpvp.2024.105422

Kumar, A., Pandey, S. M., Sirohi, S., Fydrych, D., & Pandey, C. (2023). P92 steel and inconel 617 alloy welds joint produced using ERNiCr-3 filler with GTAW process: Solidification mechanism, microstructure, mechanical properties and residual stresses. Heliyon, 9(8), e18959. https://doi.org/https://doi.org/10.1016/j.heliyon.2023.e18959

Kumar, A., Singhal, A., Sirohi, S., Hirshikesh, Fydrych, D., & Pandey, C. (2025). Pulsed current GTAW Inconel 625/AISI 304 L steel dissimilar joint: Microstructure and mechanical properties. Journal of Constructional Steel Research, 231, 109602. https://doi.org/https://doi.org/10.1016/j.jcsr.2025.109602

Kumar, N., & Kumar, P. (2024). Investigation on microstructural and mechanical integrity of GTAW dissimilar welded joint of IN 718/ASS 304L using Ni-based filler IN 625 using EBSD and DHD techniques. International Journal of Pressure Vessels and Piping, 209, 105213. https://doi.org/https://doi.org/10.1016/j.ijpvp.2024.105213

Li, S., Zhang, P., Hou, X., Wu, T., Liu, Z., Wang, X., He, P., & Arackal Narayanan, J. (2025). Weldability of rolled AlCoCrFeNi2.1/GH4169 dissimilar joints fabricated by electron beam welding. Materials Science and Engineering: A, 948, 149348. https://doi.org/https://doi.org/10.1016/j.msea.2025.149348

Li, Y.-W., Zhang, S., Zhao, J., Yu, X., & Zhang, W. (2025). Experimental study on the strength of Fe-SMA to Q355 structural steel butt welded joints. Journal of Constructional Steel Research, 226, 109277. https://doi.org/https://doi.org/10.1016/j.jcsr.2024.109277

Li, Z., Yuan, X., Yang, B., Wang, K., Zhao, Y., Sun, J., Li, J., Yang, G., Qiu, C., & Li, T. (2025). Dynamic mechanical behaviors of welded joints in power transmission construction project. Journal of Constructional Steel Research, 227, 109338. https://doi.org/https://doi.org/10.1016/j.jcsr.2025.109338

Liu, H., Fan, W., Xu, Z., Sun, C., Wu, Y., Ju, J., & Ma, J. (2025). Research progress of solid-phase welding technology between magnesium and dissimilar metals. Journal of Materials Research and Technology, 38, 5409–5440. https://doi.org/https://doi.org/10.1016/j.jmrt.2025.09.029

Liu, Y., Gong, B., Liu, S., Deng, C., Zhao, Y., Liu, Y., & Hu, W. (2025). Low-cycle fatigue properties and fracture location transition mechanism of dissimilar steel welded joints in towers of wind turbines. International Journal of Fatigue, 190, 108672. https://doi.org/https://doi.org/10.1016/j.ijfatigue.2024.108672

Ma, J., Deng, H., Liang, L., Tong, W., Wang, X., Yang, N., Wang, Z., Wen, W., Yang, L., Wu, J., & Liu, Z. (2023). Achieving superplastic TWIP steel welded joint via vacuum electron beam welding. Journal of Materials Research and Technology, 27, 1000–1016. https://doi.org/https://doi.org/10.1016/j.jmrt.2023.09.218

Maurya, A. K., B, A., Kamaraj, M., Chhibber, R., & Pandey, C. (2025). Texture corrosion resistance of SDSS 2507/Inconel 625 GTA welds: a synergistic microstructural study. Materials Chemistry and Physics, 344, 131153. https://doi.org/https://doi.org/10.1016/j.matchemphys.2025.131153

Maurya, A. K., Bhattacharyya, A., Chhibber, R., & Pandey, C. (2024). Structural integrity and corrosion behavior assessment of the dissimilar gas tungsten arc welded joint of sDSS 2507/ IN625 superalloy. Materials Chemistry and Physics, 318, 129322. https://doi.org/https://doi.org/10.1016/j.matchemphys.2024.129322

Minhas, N., Sharma, V., Manda, S., & Thakur, A. (2023). Insights into the microstructure evolution and mechanical behavior of dissimilar friction stir welded joints of additively manufactured AlSi10Mg and conventional 7075-T651 aluminum alloys. Materials Science and Engineering: A, 881, 145407. https://doi.org/https://doi.org/10.1016/j.msea.2023.145407

Naseem, A., Ilyas, M., Shehbaz, T., Hussain, G., & Alkahtani, M. (2024). Microstructural and mechanical characterization of electron beam welded low-nickel nitrogen-strengthened austenitic stainless steel. Heliyon, 10(14), e34315. https://doi.org/https://doi.org/10.1016/j.heliyon.2024.e34315

Pang, Y., Yu, H., Xia, C., Ni, C., Chen, C., Wang, S., Jia, Y., Xiao, Z., & Yi, J. (2025). Microstructural evolution and bonding mechanisms during multi-pass cold welding of high-strength precipitation-hardened alloys. Journal of Materials Processing Technology, 341, 118905. https://doi.org/https://doi.org/10.1016/j.jmatprotec.2025.118905

Salarvand, V., Ahmadian, F., Torabpour, M., EsmaeilZadeh, M., Abidi, M. H., Mehrabi, O., Sohrabpoor, H., Mostafaei, A., & Brabazon, D. (2024). Microstructure, mechanical properties, and corrosion resistance of dissimilar weld joints between SS304 and Inconel 600 welded using gas tungsten arc welding. International Journal of Pressure Vessels and Piping, 212, 105356. https://doi.org/https://doi.org/10.1016/j.ijpvp.2024.105356

Sánchez-Amaya, J. M., Chludzinski, M., Sambruno, A., & Gómez-Parra, A. (2025). Understanding the influence of different HLAW parameters to increase the welding speed of 8 mm thick structural steel. Journal of Materials Research and Technology, 39, 7217–7230. https://doi.org/https://doi.org/10.1016/j.jmrt.2025.11.058

Saravana Sundar, A., Wu, C., Li, L., Kar, A., & Kumar, A. (2025). Microstructural evolution and strengthening mechanisms in multi-pass friction stir additive manufacturing of

Al6061-Al5083 dissimilar builds: A study of overlapping thermo-mechanical zones. Journal of Materials Processing Technology, 343, 118956. https://doi.org/https://doi.org/10.1016/j.jmatprotec.2025.118956

Shotri, R., Morisada, Y., Ushioda, K., Serizawa, H., & Fujii, H. (2025). Immiscible Cu-SS304 thin tube forge welding via novel PJFW process. International Journal of Mechanical Sciences, 305, 110780. https://doi.org/https://doi.org/10.1016/j.ijmecsci.2025.110780

Sonar, T., Ivanov, M., Shcherbakov, I., Okulov, A., Shaburova, N., Liu, K., Khasanova, E., & Samoilovskikh, P. (2025). Effect of activated flux GTAW with AlCoCrFeNi2.1 eutectic high entropy alloy interlayer on microstructure and mechanical properties of dissimilar P91/304 L steel joints. Journal of Materials Processing Technology, 340, 118873. https://doi.org/https://doi.org/10.1016/j.jmatprotec.2025.118873

Tao, Z., Liu, Y., Yu, S., Gao, C., Yao, C., Wu, H., Gao, X., & Du, L. (2025). Effect of heat input on microstructural evolution and impact toughness in dissimilar weld metals between medium Mn and V-microalloyed steel. Alexandria Engineering Journal, 114, 95–111. https://doi.org/https://doi.org/10.1016/j.aej.2024.11.082

Thongsong, P., Raksat, C., Wattanajitsiri, V., & Kimapong, K. (2025). Interpass temperature control for enhancing tribological and microstructural properties of multi-pass GTAW aluminum-clad SCM440 steel. Results in Engineering, 27, 107043. https://doi.org/https://doi.org/10.1016/j.rineng.2025.107043

Tiwari, S., Kesharwani, R., Jha, K. K., Mishra, R., & Gope, P. C. (2024). Microstructural, texture, and crystallographic analysis of SiC particle incorporation in double-sided friction stir welding of dissimilar aluminium alloys. Materials Today Communications, 40, 109543. https://doi.org/https://doi.org/10.1016/j.mtcomm.2024.109543

Wang, Z., Xue, H., Hui, Y., Wang, R., Wu, J., & Zhang, Y. (2025). Investigation of crack propagation and mechanical field evolution at the tip of a growing crack under variable loading in dissimilar metal welded joints. International Journal of Pressure Vessels and Piping, 216, 105496. https://doi.org/https://doi.org/10.1016/j.ijpvp.2025.105496

Wu, C., Chen, L., Li, J., Meng, X., Guo, L., & Feng, X. (2025). Laser shock peening of 6061-T6 aluminum alloy friction stir welding joints: Microstructure evolution, fracture morphology and strengthening mechanism. Journal of Materials Research and Technology, 39, 3981–3998. https://doi.org/https://doi.org/10.1016/j.jmrt.2025.10.103

Yadav, J., Gangil, N., Siddiquee, A. N., Ali Mohsin, M. E., Alnamasi, K., Moinuddin, S. Q., Khan, M. F., & Maheshwari, S. (2025). Effect of tool pin profiles on defects formation during friction stir welding of AA 6082-T6 straight-pipes-butt-weld joints. Journal of Materials Research and Technology, 36, 1645–1657. https://doi.org/https://doi.org/10.1016/j.jmrt.2025.03.185

Yang, J., Dong, H., Wu, G., & Xiong, F. (2025). Experimental and numerical simulation study on microstructure, residual stress and mechanical properties of Fe–Mn–C–Cr cryogenic high-manganese steel arc-welded joint. Journal of Materials Research and Technology, 35, 1335–1347. https://doi.org/https://doi.org/10.1016/j.jmrt.2025.01.114

Yang, Y., Huang, X., Yu, X., Wang, S., & Ji, H. (2024). Comparative analysis of welding quality in Q235/20# dissimilar steel: Intermittent vs. full TIG welding. Journal of Materials Research and Technology, 33, 8768–8779. https://doi.org/https://doi.org/10.1016/j.jmrt.2024.11.191

Yelamasetti, B., Devi, B. T. L., Saxena, K. K., Sonia, P., Vardhan, T. V., Sree, N. S., khubnani, R., Abdo, H. S., & Alnaser, I. (2024). Mechanical characterization and microstructural evolution of Inconel 718 and SS316L TIG weldments at high temperatures. Journal of Materials Research and Technology, 32, 196–207. https://doi.org/https://doi.org/10.1016/j.jmrt.2024.07.157

Yelamasetti, B., Phani Sushma, I. S., Radha, K. K., Zubairuddin, M., Sharma, S., Arunachalam, K. P., Ismail, A. I., & Ramaswamy, K. (2025). Investigation of thermal fields, residual stresses, and tensile strength of dissimilar weldments of AA5052-AA7075 alloys on the stress corrosion cracking: Comparative analysis of coolant effects for enhancing weld integrity. Journal of Materials Research and Technology, 38, 6315–6326. https://doi.org/https://doi.org/10.1016/j.jmrt.2025.09.032

Yu, J., Zhang, H., Wang, B., Du, R., Fan, Y., & He, P. (2023). Interfacial evolution behavior and mechanical properties of Ti/steel joint via ultrasonic seam assisted resistance spot welding with Cu interlayer. Journal of Manufacturing Processes, 95, 535–550. https://doi.org/https://doi.org/10.1016/j.jmapro.2023.03.081

Zhang, B., Ning, Y., Wang, Z., Li, M., Xie, B., & Liu, Q. (2024). Interface microstructural evolution, microhardness variation mechanism and 750 °C tensile behavior of the HIPed/FGed PM superalloy plastic bonded joints. Journal of Materials Research and Technology, 30, 8938–8951. https://doi.org/https://doi.org/10.1016/j.jmrt.2024.05.259

Zhang, Q., Xu, J., Wu, B., Wang, Q., Wang, X., Zhang, Z., & Zhou, H. (2025). Influence of transverse residual stress and welding defect on fracture performance of thick weld based on GTN damage model. International Journal of Naval Architecture and Ocean Engineering, 17, 100654. https://doi.org/https://doi.org/10.1016/j.ijnaoe.2025.100654

Zhang, Y., Fang, C., Wang, W., & Hou, H. (2023). Cyclic plasticity and ULCF behavior of steel butt-joints considering different welding methods. International Journal of Fatigue, 173, 107684. https://doi.org/https://doi.org/10.1016/j.ijfatigue.2023.107684

Zhou, X., Li, R., Liu, F., Wang, B., Wei, L., Tian, L., Yang, M., Song, X., & Tan, C. (2024). Microstructure evolution and corrosion behavior improvement of oscillation laser welded 2205/316L dissimilar joints used in offshore platform. Ocean Engineering, 311, 118833. https://doi.org/https://doi.org/10.1016/j.oceaneng.2024.118833

Zhu, Q. L., Yu, J. M., Xu, C., Li, X., Zhang, Z. H., Hu, Z. R., Wang, X. N., & Nagaumi, H. (2025). Advancing near-infrared and blue hybrid laser welding: Energy efficiency and microstructural refinement in Al-Mg-Si dissimilar joints. Journal of Materials Processing Technology, 340, 118842. https://doi.org/https://doi.org/10.1016/j.jmatprotec.2025.118842